Journal of Physics: Conference Series **3224** (2026) 032032 doi:10.1088/1742-6596/3224/3/032032

A multi-Gaussian wake modelling method for a lateral row of turbines

Zheni Fei[1], **Christopher R. Vogel**[1] **and Takafumi Nishino**[1]

[1]Department of Engineering Science, University of Oxford, Oxford, United Kingdom

E-mail: zheni.fei@eng.ox.ac.uk

Abstract. Calculating the wake behind multiple turbines has been a challenge in wake modelling. Superposition methods have been widely used because of their simplicity. However, it is hard to truly conserve momentum using these techniques. Momentum-conserving models also do not usually consider how wake interactions affect the recovery rate. Thus, these models do not always provide accurate predictions. In this study, we propose a new far-wake model for a lateral row of identical turbines in a uniform flow that accounts for the reduction of lateral transfer of energy between neighbouring turbine wakes. The model assumes a multi-Gaussian wake profile and models the recovery rate by calculating the divergence of the Reynolds shear stresses. We verify the model with numerical simulations of flow past actuator discs over a range of thrust coefficients, inflow turbulence intensities and two turbine spacings, and also compare it with linear and root-sum-square superposition methods of a single wake. Overall, the proposed model demonstrates good agreement with the simulation results. This new approach could provide a basis for engineering modelling of wind farm internal flow fields and multi-rotor turbine wakes in future studies.

1. Introduction

As wind farms grow in size, some turbines are likely to operate in the wake of other turbines. The wake effect is known to decrease the power available for extraction by the downstream turbines; thus, good wake prediction is crucial for wind farm design and optimisation. Since high-fidelity models, such as Large Eddy Simulations (LES), are too expensive for farm layout optimisation, engineering wake models are often used for farm design. Frequently used models include the Jensen model [1], Bastankhah and Porté-Agel (BP) model [2], and the Ainslie model [3]. These models were developed for single turbines and require a wake merging method to predict the wake of multiple turbines.

The most widely used wake merging method is the superposition method. Two common methods are the linear superposition method and the root-sum-square (RSS) superposition method. Linear superposition is based on the assumption that the velocity deficit is analogous to a passive scalar plume in the far-wake region [4]. Thus, the resultant wake can be modelled by directly superimposing the individual wakes. RSS superposition assumes that the kinetic energy deficit of the merged wake is the sum of the energy deficit of individual wakes. There are also different definitions of the velocity deficit of the turbine wakes. Some models define it with respect to the freestream, and some models define it with respect to the flow generated by the upstream turbine. While the superposition methods do not necessarily conserve physical

quantities such as mass and momentum, some models give good accuracy under certain conditions. More recent wake merging methods better conserve momentum ([5], [6]), but lack consideration of how wake-wake interactions change the wake recovery rate.

There are two main mechanisms of how wake interaction affects wake recovery. One is to increase turbulence intensity through wake-induced turbulence. This mechanism is usually considered by modifying the wake expansion rate in the single wake model. Another mechanism is related to the energy available for wake re-energisation: when two side-by-side wakes interact, they compete for the energy for wake recovery. This mechanism is rarely considered in existing models.

In this study, we propose a new far-wake model that considers the competing effects between wakes. Here, we formulate the model to predict the far wake development behind a lateral row of turbines. Instead of superimposing the wake of an individual turbine, we predict the wake evolution from its main driving forces and consider the combined wake as a whole. We evaluate the proposed model under different inflow turbulence intensities, thrust coefficients, and turbine spacings. The model can be used to calculate multi-rotor turbine wake and has the potential to be further developed for wind farm velocity field modelling.

The paper is structured as follows. Section 2 introduces the theoretical basis of the model and how it can be implemented; Section 3 describes the setup of the numerical simulation used to verify the model; Section 4 shows the model results and analyses the underlying mechanisms, and Section 5 concludes the study.

2. Analytical model

2.1. Problem definition

In this study, we consider a lateral row of n turbines placed in a uniform flow with velocity U_0 as shown in Figure 1. All the turbines are identical and exert the same thrust. The turbine hub-to-hub spacing is S and is set to $2D$ for a range of inflow turbulence intensities and thrust coefficients, where D is the turbine diameter. We also studied a reduced separation case where $S = 1.2D$ for inflow turbulence intensity of 10% and a thrust coefficient of 0.6259. We assume the wake of each turbine is also identical, and thus can be defined by the same wake centre

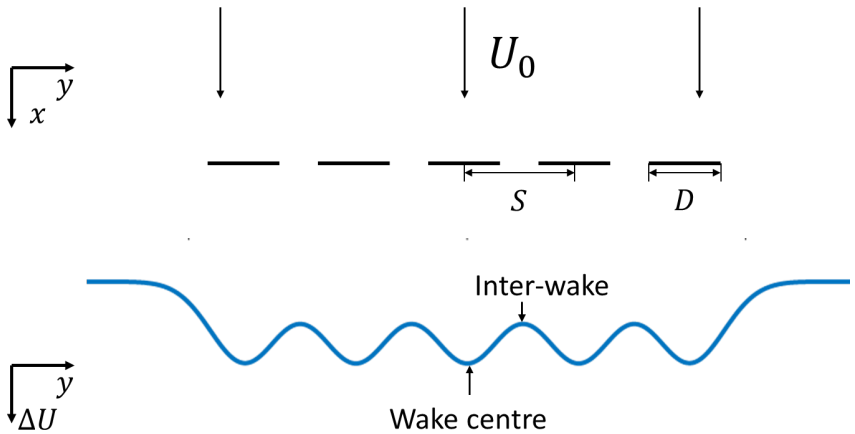

Figure 1. An array of turbines experiencing uniform inflow (top) and its far-wake wake profile (bottom).

velocity deficit C and characteristic width σ, so that the wake velocity, U, has the form

$$\frac{U}{U_0} = 1 - \sum_{i=1}^{n} C e^{-\frac{(y-Y_i)^2+(z-Z_i)^2}{2\sigma^2}}, \tag{1}$$

where y and z are the horizontal and vertical coordinates, respectively, Y_i and Z_i are the horizontal and vertical positions of each turbine, respectively. Although the model can handle varying Z_i in principle to model the wake of a multi-rotor turbine [7], we consider the scenario where Z_i for all turbines are identical. We set n to be 5 in this study, so that the wake profile is as shown in the bottom sketch in Figure 1. We solve the streamwise evolution of the wake centre velocity at the position marked in Figure 1, and calculate the velocity profile by Equation 1. We neglect the finite array effect, which would cause each turbine to experience slightly different inflow velocity.

2.2. Driving forces for wake recovery

We find the main driving forces of wake recovery by examining the streamwise component of the steady Reynolds-Averaged Navier-Stokes (RANS) equations given as

$$U\frac{\partial U}{\partial x} + V\frac{\partial U}{\partial y} + W\frac{\partial U}{\partial z} = -\frac{1}{\rho}\frac{\partial p}{\partial x} + \nu\left(\frac{\partial^2 U}{\partial x^2} + \frac{\partial^2 U}{\partial y^2} + \frac{\partial^2 U}{\partial z^2}\right) - \frac{\partial \overline{u'u'}}{\partial x} - \frac{\partial \overline{u'v'}}{\partial y} - \frac{\partial \overline{u'w'}}{\partial z}, \tag{2}$$

where V, W are spanwise (y) and vertical (z) mean velocities, respectively, x is the streamwise coordinate, p is static pressure, ρ is fluid density, and $\overline{u'u'}$, $\overline{u'v'}$, $\overline{u'w'}$ are the streamwise, spanwise and vertical components of the Reynolds stresses, respectively, and ν is the kinematic viscosity. We then use the Boussinesq (linear) eddy viscosity hypothesis which states

$$\overline{u'u'} = \frac{2}{3}k - 2\nu_t\frac{\partial U}{\partial x}, \quad \overline{u'v'} = -\nu_t\left(\frac{\partial U}{\partial y} + \frac{\partial V}{\partial x}\right), \quad \overline{u'w'} = -\nu_t\left(\frac{\partial U}{\partial z} + \frac{\partial W}{\partial x}\right), \tag{3}$$

where ν_t is the kinematic eddy viscosity, and k is the turbulent kinetic energy. Along the wake centre of the central turbine, $V\frac{\partial U}{\partial y} = W\frac{\partial U}{\partial z} = 0$ due to symmetry, ν is much smaller than ν_t, and we assume that $\frac{\partial \overline{u'u'}}{\partial x}$, $\nu_t\frac{\partial^2 V}{\partial x \partial y}$ and $\nu_t\frac{\partial^2 W}{\partial x \partial z}$ are relatively small compared to the other terms. Therefore, Equation 2 for the wake centreline can be reduced to

$$\alpha\frac{\partial \alpha}{\partial \hat{x}} = -\frac{\partial \hat{p}}{\partial \hat{x}} + \mathcal{R}, \tag{4}$$

where $\hat{p} = p/(\rho U_0^2)$, $\hat{\nu}_t = \nu_t/(U_0 D)$, $\hat{x} = x/D$, $\hat{y} = y/D$, $\hat{z} = z/D$, and $\mathcal{R} = \hat{\nu}_t(\frac{\partial^2 \hat{U}}{\partial \hat{y}^2} + \frac{\partial^2 \hat{U}}{\partial \hat{z}^2})$, $\hat{U} = U/U_0$, and α is $\hat{U}$ at the wake centre. In the far-wake region, the pressure gradient term is negligible, so Equation 4 can be simplified to

$$\alpha\frac{\partial \alpha}{\partial \hat{x}} = \mathcal{R}. \tag{5}$$

This implies that, at the axis of symmetry, the main recovery mechanism in the far wake is the divergence of the Reynolds shear stresses. This idea is stressed by van der Laan et al. [8], and is also an assumption of the Ainslie model [3], which solves a simplified streamwise component of the RANS equations numerically. By assuming the wake profile is Gaussian, a simplified solution can also be derived [9], which solves the wake centreline velocity by an ordinary differential equation.

The Ainslie model [3] and its simplified version [9] are both single-wake models. The main difference between a single turbine and a cross-stream row of turbines is that, for a single wake, the energy transport occurs both in vertical and horizontal directions. In the case of a row of turbines, in the region close to the turbines before wakes have merged, each wake may still entrain some energy from the horizontal direction. As the wakes start to merge, each wake entrains the majority of the energy vertically. We can capture this change in the energy entrainment using Equation 5 and the wake profile described by Equation 1.

2.3. Turbine row model

To solve how the velocity develops in the far-wake region, we rearrange Equation 5 to

$$\frac{\partial \alpha}{\partial \hat{x}} = \frac{\mathcal{R}}{\alpha}. \tag{6}$$

Then we define a series of infinitesimal control volumes along the wake centreline and integrate this equation from the inlet to the outlet of each control volume. Using a first-order Taylor expansion, we have

$$\alpha_{i+1} = \alpha_i + \frac{\mathcal{R}}{\alpha_i}\Delta\hat{x} \tag{7}$$

where α_i is α at the inlet of the i-th control volume.

The proposed multi-Gaussian model solves the wake using the following process.

1. Pick a position $\hat{x}_0$ where we start the far wake modelling, and give the wake centre velocity α_0 at this point. In this study, we extract α_0 directly from the numerical simulation (against which the far wake model is validated).
2. Calculate the corresponding wake width σ by inserting Equation 1 into the conservation of momentum equation,
$$\int_{A_c} U(U_0 - U)dA = \frac{T}{\rho}, \tag{8}$$
where A_c is the domain size averaged on the central turbine and has the width of S, and T is the thrust of a single turbine.
3. Calculate $\mathcal{R}$ using the velocity profile determined by Equation 1.
4. Iterate the solution using Equation 7.
5. Use α_{i+1} and Equation 8 to calculate σ_{i+1}, to give the new velocity profile.
6. Repeat steps 3 to 5 until the entire wake is solved.

2.4. Single wake model and superposition methods

To compare with the conventional superposition methods, we use a single wake model derived by Anderson [9] and two superposition methods. We choose the Anderson model as the single wake model because it also predicts the wake evolution by calculating the divergence of the Reynolds shear stresses from the assumed wake profile, and requires the same type of input as the proposed multi-Gaussian model. The Anderson model [9] has the form of

$$\frac{d\alpha}{d\hat{x}} = \frac{16\hat{\nu}_t(\alpha^3 - \alpha^2 - \alpha + 1)}{\alpha C_t}, \tag{9}$$

where C_t is the thrust coefficient. The superposition methods used are linear superposition

$$\hat{U} = 1 - \sum_{i=1}^{n}(1 - \hat{U}), \tag{10}$$

and RSS superposition

$$\hat{U} = 1 - \sqrt{\sum_{i=1}^{n}(1-\hat{U})^2} \tag{11}$$

In this study, we are mainly interested in the wake evolution in the far-wake region and the mechanism of wake recovery. Thus, we take the wake centreline velocity from the simulation at a selected starting point $\hat{x}_0$ and the eddy viscosity along the wake centre, and use them as inputs to the multi-Gaussian model and the Anderson model [9]. The results from the Anderson model are then combined with different superposition methods to predict the row wake.

3. Numerical simulation

In the current study, we compare the wake centreline velocity and a newly defined velocity deficit of the central turbine with RANS simulations of a turbine in an infinitely wide row, achieved using symmetry boundary conditions. We make this comparison because the analytical model predictions using five turbines and seven turbines were almost identical, which suggests that adding more turbines would not significantly change the model prediction.

3.1. Governing equations

Three-dimensional RANS simulations with a modified k-ϵ turbulence model have been performed using OpenFOAM to verify the proposed wake model. The RANS actuator disc code for representing the turbine is adapted from the original code by Svenning [10], which has been validated by the data from Mikkelsen [11].

To maintain the turbulence level in the uniform background flow, we add a pair of source terms to the standard $k-\epsilon$ turbulence model. The $k-\epsilon$ model in OpenFOAM solves

$$\frac{D}{Dt}(\rho k) = \nabla\cdot(\rho D_k \nabla k) + P - \rho\epsilon + S_k \tag{12}$$

and

$$\frac{D}{Dt}(\rho\epsilon) = \nabla\cdot(\rho D_\epsilon \nabla\epsilon) + \frac{C_1\epsilon}{k}(P + C_3\frac{2}{3}k\nabla\cdot\vec{u}) - C_2\rho\frac{\epsilon^2}{k} + S_\epsilon, \tag{13}$$

where t is time, D_k is the eddy diffusivity for k, P is the turbulent kinetic energy production rate, S_k is the source term for k, ϵ is the turbulent kinetic energy dissipation rate, D_ϵ is the effective diffusivity for ϵ, C_1, C_2 and C_3 are all model coefficients, $\vec{u}$ is the velocity vector, and S_ϵ is the source term for ϵ. For the standard implementation of the $k-\epsilon$ model, both S_k and S_ϵ equal zero. In this study, we used the 'scalarSemiImplicitSource' function in OpenFOAM to add the source terms, so that the turbulence does not decay in uniform flow. The two source terms are

$$S_k = \rho\epsilon \tag{14}$$

and

$$S_\epsilon = C_2\rho\frac{\epsilon^2}{k}. \tag{15}$$

The same approach was previously used by van der Laan et al. [12].

3.2. Simulation setup

The turbine is represented by an actuator disc placed $15D$ downstream from the inlet and $50D$ upstream from the outlet of a rectangular computational domain, with a cross-section of $2D \times 27.5D$ for $S = 2D$, and $1.2D \times 27.5D$ for $S = 1.2D$. No hub or support structure is simulated, and the tangential force is turned off to yield the simplest case of the disc, reducing only the axial momentum of the flow.

Table 1. Parameters for the simulation cases.

	cases 1-4				cases 5-7		
$Ti(\%)$	1	5	10	20	10		
C_t	0.6259				0.36	0.75	0.8889

Table 2. Summary of simulation boundary conditions.

	Inlet	Outlet	Sidewalls
U	fixed value (10 m/s)	zero gradient	slip
p	zero gradient	fixed value	zero gradient
k and ϵ	fixed value	zero gradient	zero gradient

The 'blockmesh' function in OpenFOAM was used to generate multi-block structured grids with hexahedral cells. In the streamwise direction, the mesh is refined near the disc and expands in the downstream direction. A refined region for the disc is meshed independently, and the actual disc ($0.025D$ thick) is located in the middle of the refined region ($0.03D$ thick). The mesh in this region is very fine (with 12 cells being uniformly distributed across the $0.03D$-thick region) to make sure that the volume force exerted is accurate and does not change in the mesh convergence study.

This baseline mesh was refined using the 'SnappyHexMesh' function in OpenFOAM to obtain three additional meshes for a mesh convergence study. The refinement level is defined such that level m divides each cell in the baseline mesh into 2^m parts in each direction. As a compromise between accuracy and computational cost, refinement level 1 is adopted in this study. The final mesh consists of 2,765,824 hexahedral cells for $S = 2D$, and 2,691,072 cells for $S = 1.2D$. The sizes of the cells near the disc are $0.05D$ in the tangential direction and $0.021D$ in the radial direction.

For all the cases simulated, the Reynolds number, defined as $Re = \frac{U_0 D}{\nu}$, is 2.67×10^7. The mixing length l at the inflow is 10 m. A range of inflow turbulence intensities and thrust coefficients for $S = 2D$ is simulated and summarised in Table 1, where Ti is the inflow turbulence intensity. For $S = 1.2D$, $C_t = 0.6259$ and $Ti = 10\%$. The boundary conditions are summarised in Table 2. The inlet k is calculated from Ti as $1.5(TiU_0)^2$, and the corresponding inlet ϵ is calculated as $C_\mu^{0.75} k^{1.5}/l$, where C_μ is a model constant equal to 0.09.

4. Results

4.1. Centreline velocity

Figure 2 shows the wake centreline velocity of the simulation and different model predictions for varying thrust coefficients. The discrepancies between different models for $C_t = 0.36$ are negligible. This is expected, since a small thrust coefficient leads to a small wake deficit, and the wake interaction is trivial. As the thrust coefficient increases, the wake interaction gets stronger, and differences between the models emerge. As expected, the single wake model predicts a faster recovery rate, since the model allows the wake to entrain energy from both the vertical and the horizontal directions equally. The multi-Gaussian has the slowest recovery rate because it limits the energy transfer along the horizontal direction. Linear superposition has a slower recovery rate than RSS method because its calculated velocity deficit scales with $\sqrt{n}\Delta U$, while the velocity deficit calculated by the linear superposition scales with $n\Delta U$, where ΔU is the velocity deficit of a single turbine. A similar trend was observed by Vogel and Willden [13]. The overall

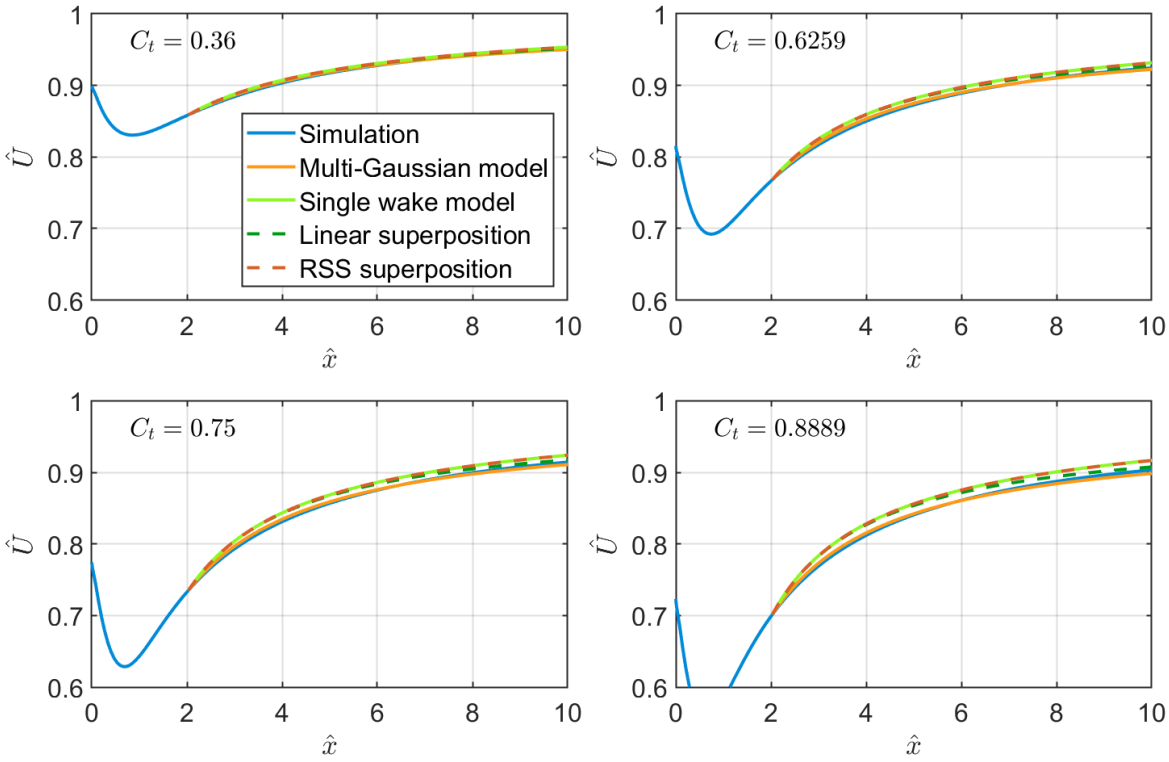

Figure 2. Comparison of wake centreline velocity between simulation results and different models for a range of thrust coefficients.

better agreement of the proposed multi-Gaussian model demonstrates that modelling the non-negligible interactions between neighbouring wakes is important for predicting the recovery of multiple wakes.

The results for varying inflow turbulence intensities are shown in Figure 3. For $Ti = 1\%$, the velocities predicted by both linear superposition and RSS superposition are almost identical to the wake predicted by the single wake model. This is because the models predict that the wake expands slowly for low turbulence conditions, and the wake interaction is weak. For higher turbulence intensities, the linear superposition method predicts a slower recovery rate than the RSS method, which suggests that the wake interaction gets stronger. The multi-Gaussian model still predicts the slowest recovery rate, and has the most accurate solution except for $Ti = 20\%$. For $Ti = 20\%$, the multi-Gaussian slightly underestimates the velocity compared to the simulations. This is partly because the model only considers the velocity deficit and ignores the velocity increase in the bypass due to conserved mass flux. Additionally, as the inflow turbulence intensity increases, the multi-Gaussian model changes from overestimating the recovery rate to underestimating the recovery rate. This transition is related to how inflow turbulence intensity changes the wake profile.

4.2. Velocity deficit at the turbine scale

The centreline velocity corresponds to the conventional velocity deficit, C, and represents wake recovery with respect to the velocity far upstream. We are also interested in how the individual

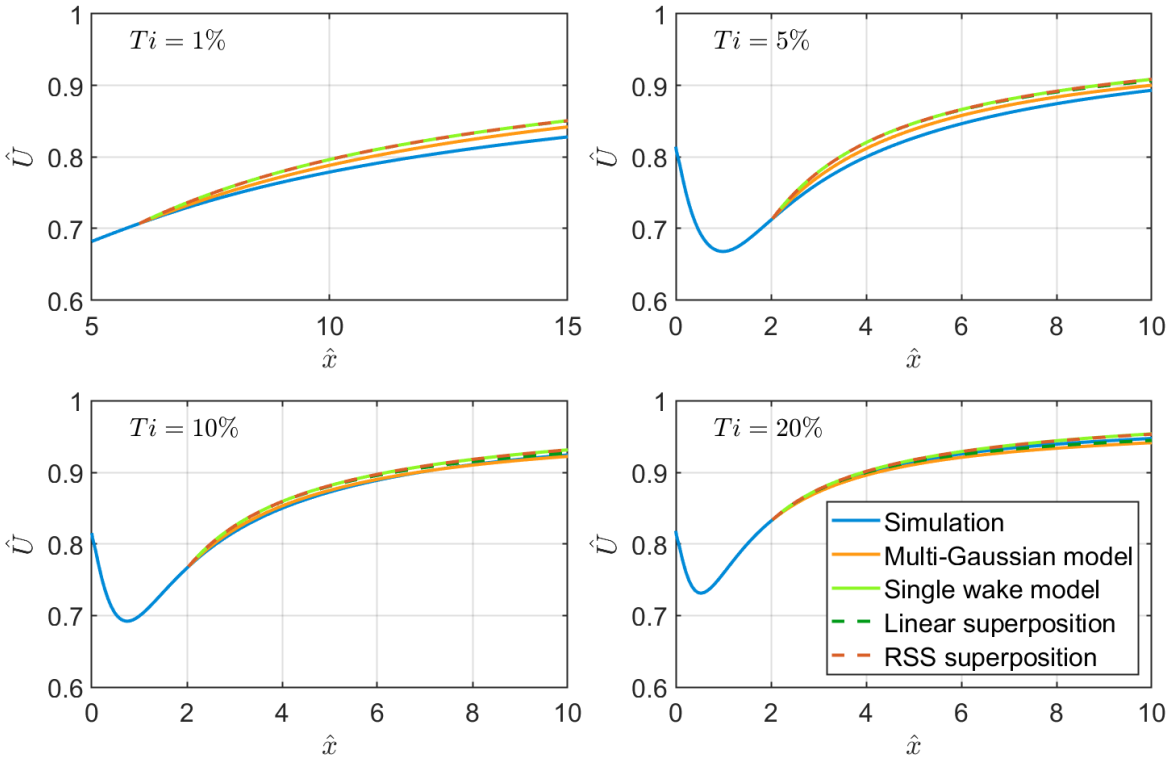

Figure 3. Comparison of wake centreline velocity between simulation results and different models for a range of inflow turbulence intensities.

wake recovers within the array. We define

$$\delta U = U_{iw} - U_{wc}, \tag{16}$$

where U_{iw} is the velocity at the inter-wake position and U_{wc} is the velocity at the wake centre position as shown in Figure 1. δU is the velocity deficit at the turbine scale within the array, and measures the wake profile variation. However, directly using δU for different models does not give the best comparison of how fast the wake profile changes, because there is a discrepancy between the Gaussian wake profile and the experimental wake profile for a single turbine, as described by Pope [14]. This discrepancy, observed mostly around the wake edges, is partly attributed to the non-uniformity in eddy viscosity in the spanwise direction. This argument is supported by the simulation results of van der Laan et al. [8], who showed that a uniform eddy viscosity leads to a wake profile closer to a Gaussian shape. For multiple wakes merged together, this discrepancy manifests in a lower velocity at the inter-wake position. Thus, all models have a smaller δU than the simulation at the starting position of far-wake modelling, where all the models start with the same centreline velocity as the simulation. Since different models underestimate the inter-wake velocity by different amounts, we normalise δU by δU_0, where δU_0 is δU at the starting position. $\delta U/\delta U_0$ reflects the proportion of the (individual) wake deficit that has not been recovered, and better represents how fast the wake profile varies.

Figure 4 shows $\delta U/\delta U_0$ from simulation and different model results for a range of thrust coefficients and inflow turbulence intensities. For all the thrust coefficients examined, the single wake model underestimates the profile variation rate because there is no wake merging at all. RSS superposition also underestimates the profile variation rate, because it considers

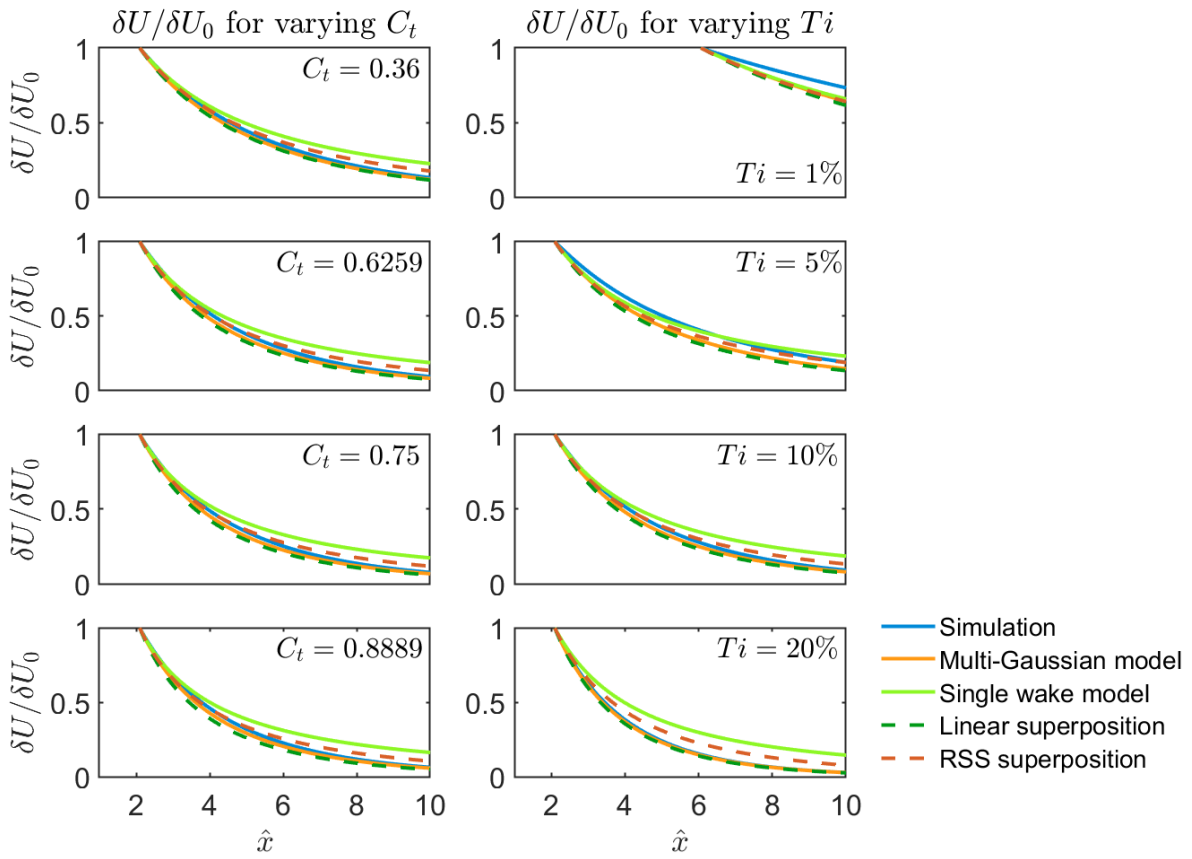

Figure 4. Comparison of $\delta U/\delta U_0$ between simulation results and different models for a range of thrust coefficients and inflow turbulence intensities.

a weaker wake interaction compared to the linear superposition and the multi-Gaussian wake models. Both the proposed multi-Gaussian model and the linear superposition method show good agreement with the simulation results, and it captures accurate variation in terms of the change in wake profile.

For different inflow turbulence intensities, all models overestimate the profile variation rate at $Ti = 1\%$. This is because, for low turbulence intensity, a Gaussian profile tends to predict a wider wake width, which corresponds to stronger wake interaction, and the profile variation rate is faster. This effect gradually disappears as the inflow turbulence intensity increases. At $Ti = 5\%$, the single wake model and RSS method show better agreement with the simulation, but as the turbulence intensity increases, these two models gradually switch from overestimation to underestimation of the profile variation rate; hence, this better agreement may be coincidental. The linear superposition method and the proposed multi-Gaussian model still have similar results. Their agreement with the simulation increases as the turbulence intensity increases. This implies that the wake interaction for $S = 2D$ is quite weak, and the momentum deficit behaves similarly to a passive scalar.

4.3. Computational cost and multi-rotor turbine application

The computational cost required for the proposed multi-Gaussian method is on the order of seconds, which is a few orders of magnitude higher than the superposition methods (10^{-4} to

10^{-3} s), but it is still much lower than the cost for RANS simulations (10^3 to 10^4 s). Although the multi-Gaussian model shows modest improvement over the linear superposition approach, it captures key wake-recovery mechanisms and provides a physically consistent framework, whereas the linear superposition method, although computationally efficient and accurate for the cases considered, can occasionally yield non-physical solutions.

We examine the physical consistency of the proposed model with a much smaller rotor spacing typical for a multi-rotor turbine [7], which has stronger wake interaction, $S = 1.2D$, which corresponds to a turbine tip-to-tip spacing of $0.2D$. The results are shown in Figure 5. In this case, the difference between the single wake model and the simulation wake centreline velocities is much larger compared to the case of $S = 2D$, which implies stronger wake interaction. Both the multi-Gaussian model and the linear superposition method predict wake centreline velocity in good agreement with the simulation results. The RSS superposition improves little from the single wake model in terms of wake centreline velocity. For $\delta U/\delta U_0$, both the linear superposition and the multi-Gaussian models agree well with the simulation $\delta U/\delta U_0$ up to $8D$. Downstream of $8D$, both the multi-Gaussian model and the RSS model predict $\delta U/\delta U_0$ tends to zero in consistency with the simulation results, while the linear superposition predicts an increasing $\delta U/\delta U_0$. This increasing $\delta U/\delta U_0$ arises from the fact that the linear superposition predicts a faster recovery rate at the inter-wake position than that along the wake centreline downstream of $8D$. Thus, although both the linear superposition method and the multi-Gaussian model yield good agreement with the simulation results in terms of wake centreline velocity, the multi-Gaussian model provides a more physically consistent solution and has more potential to deal with more complex wake interactions.

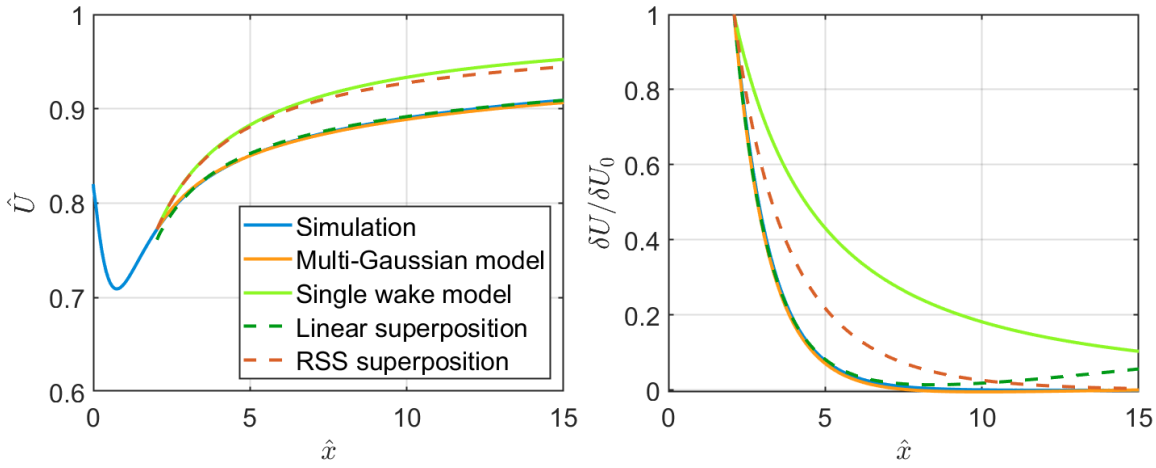

Figure 5. Comparison of centreline velocity and $\delta U/\delta U_0$ between simulation results and different models for $C_t = 0.6259$, $Ti = 10\%$ and $S = 1.2D$.

5. Conclusions

This study presents an analytical model that employs a multi-Gaussian wake profile to predict the wake recovery downstream of a lateral row of turbines, accounting for the reduction of lateral energy transfer between neighbouring wakes. The proposed model is compared with single-turbine model predictions and results from superposition methods, and validated against RANS simulations. We evaluated the model performance using wake centreline velocity and the velocity difference between the wake centre and the inter-wake positions.

For most flow conditions, the RSS method overpredicts the centreline velocity recovery and underpredicts the wake profile variation rate compared to RANS simulations, which corresponds to underestimating the interactions between neighbouring wakes. For different thrust coefficients and inflow turbulence intensities at $S = 2D$, the multi-Gaussian model agrees better with the simulations compared to the single wake model, despite the small discrepancy between the single wake model and the simulation. The linear superposition method also demonstrates good agreement and retains an advantage in computational cost over the multi-Gaussian model. However, under strong wake interaction at $S = 1.2D$, it can yield non-physical solutions, whereas the multi-Gaussian formulation maintains physical consistency and predictive robustness.

Overall, the proposed multi-Gaussian framework demonstrates potential for modelling wake interactions behind a lateral row of turbines, including multi-rotor systems at substantially reduced computational cost relative to CFD simulations. For more general turbine layouts, further developments are required, including the ability to model different wake centreline velocity deficits and wake characteristic widths for individual wakes and the incorporation of a near-wake model for turbines operating within each other's induction zone.

Acknowledgments
This work was partly supported through CRV's UKRI Future Leader's Fellowship MR/V02504X/1.

References

[1] Jensen N O 1983 A note on wind generator interaction *Tech. Rep. Risø-M-2411* **2411**
[2] Bastankhah M and Porté-Agel F 2014 A new analytical model for wind-turbine wakes *Renewable Energy* **70** 116–123
[3] Ainslie J F 1988 Calculating the flowfield in the wake of wind turbines *Journal of Wind Engineering and Industrial Aerodynamics* **27** 213–224
[4] Lissaman P B 1979 Energy effectiveness of arbitrary arrays of wind turbines *Journal of Energy* **3** 323–328
[5] Bastankhah M, Welch B L, Martínez-Tossas L A, King J and Fleming P 2021 Analytical solution for the cumulative wake of wind turbines in wind farms *Journal of Fluid Mechanics* **911** A53
[6] Zong H and Porté-Agel F 2020 A momentum-conserving wake superposition method for wind farm power prediction *Journal of Fluid Mechanics* **889** A8
[7] Bastankhah M and Abkar M 2019 Multirotor wind turbine wakes *Physics of Fluids* **31**
[8] van der Laan M P, Baungaard M and Kelly M 2022 Brief communication: A clarification of wake recovery mechanisms *Wind Energy Science Discussions* **2022** 1–8
[9] Anderson M 2009 Simplified solution to the eddy-viscosity wake model *Tech. Rep. Global Renewable Energy Solution company*
[10] Svenning E 2010 Implementation of an actuator disk in OpenFOAM *Chalmers University of Technology*
[11] Mikkelsen R 2003 *Actuator disc methods applied to wind turbines* Ph.D. thesis Technical University of Denmark
[12] Van der Laan M, Hansen K S, Sørensen N N and Réthoré P E 2015 Predicting wind farm wake interaction with RANS: an investigation of the Coriolis force *Journal of Physics: Conference Series* **625** 012026
[13] Vogel C R and Willden R H 2020 Investigation of wind turbine wake superposition models using Reynolds-Averaged Navier-Stokes simulations *Wind Energy* **23** 593–607
[14] Pope S B 2000 *Turbulent flows* (Cambridge University Press)